Optical Chemical Sensor and Electronic Nose Based on Porphyrin and Phthalocyanine

Teerakiat Kerdcharoen and Sumana Kladsomboon

Abstract Recently, electronic nose (e-nose) has emerged as a viable technology to detect and analyze various kinds of gases based on chemical gas sensor array and pattern recognition. Researchers worldwide make their efforts to improve the sensitivity and stability of the chemical gas sensors. Among the sensing and transduction technologies, such as metal oxide, piezoelectric, organic semiconductor, nano-composite and optical sensing, optical gas sensors present several advantages, i.e., low energy consumption and high signal-to-error ratio, etc. Specifically, the optical gas sensors based on optically active organic materials, e.g., metallo-porphyrin (MP) and metallo-phthalocyanine (MPc) molecules, have recently become very attractive and practically alternative because MP and MPc present versatile and tunable optical spectra by changing the central metal atoms such as Zn and Mg. For this type of gas sensors, an ordinary UV–Vis spectrophotometer can be easily modified to be the transducing unit for optical e-nose measurement. The gas sensing films were prepared by spin-coating and working by measuring the absorption spectral change under ambient conditions. A simple pattern recognition method such as principal component analysis (PCA) was demonstrated to be very effective for this e-nose system. The results from the PCA method indicate that both MP and MPc materials were cost-effective choices for classifying various odors. Based on the density functional theory (DFT) calculations, sensing mechanism of this type of chemical sensors can be described in terms of the ion–dipole interactions between the central metals of the sensing molecules and VOCs molecule.

Keywords Chemical gas sensors, Electronic nose, Optical gas sensors, Porphyrin and phthalocyanine

T. Kerdcharoen (✉) and S. Kladsomboon
Faculty of Science, Department of Physics, Mahidol University, Bangkok, Thailand
e-mail: sctkc@mucc.mahidol.ac.th

A. Tuantranont (ed.), *Applications of Nanomaterials in Sensors and Diagnostics*,
Springer Series on Chemical Sensors and Biosensors (2013) 14: 237–256
DOI 10.1007/5346_2012_49,
Published online: 18 March 2013

Contents

1 Introduction

Chemical gas sensor is a device that converts chemical properties of the odorants into electronic signal. There are many types of chemical gas sensors, for instance, conductometric, gravimetric (piezoelectricity), chemoresistor, and optical sensor. Among these transduction techniques, optical measurement has been one of the most popular choices due to its variety in the measurement of optical modes, for example, absorbance, fluorescence, polarization, refractive index, and reflectance [1, 2]. Metallo-porphyrin (MP) and metallo-phthalocyanine (MPc), which are the organic compounds, have been very attractive sensing materials because their absorption spectral changes upon exposure to volatiles are active in the visible region [3]. Consequently, measuring the color changes within the absorption spectra of these sensing materials can be done conveniently using standard instrument such as UV–Vis spectrophotometer. Such equipment can be modified to incorporate gas flow chamber, data acquisition, and processing, which finally leads to an optical electronic nose system that can effectively discriminate organic compounds (VOCs) in the aroma of food and beverages [4]. The optical e-nose system developed from a general UV–Vis spectrophotometer has thus become a promising new technology for odor classification for food and agricultural industries.

This chapter is divided into six sections as follows: (1) introduction, (2) chemical gas sensor, (3) a background on porphyrin and phthalocyanine, (4) e-nose system based on UV–Vis spectrophotometer, (5) development of optical gas sensor, and (6) odor classification based on principal component analysis (PCA).

2 Chemical Gas Sensor

e-Nose has become a new technology for odor classification by mimicking the functions of the olfactory system in human. In the olfactory system, there are millions of odorant receptors in the nasal working for odor detection. Signals

from the odorant receptors are accumulated and transmitted to the brain by the olfactory bulb. Then, the brain classifies the odor types using pattern recognition based on the past memory. In turn, an e-nose system consists of a gas sensor array, signal processing, and pattern recognition, reflecting the biological odorant receptors, olfactory bulb, and brain, respectively [4]. The most important area in the development of e-nose is to improve the sensitivity and stability of the chemical gas sensors.

In contrast to biological nose that involves very complex biological and neural process, odor sensing in e-nose is based on much simpler transduction techniques such as electrochemical, optical, and gravimetric approaches. Electrochemical transduction, as often implemented in the metal-oxide semiconductor gas sensor, is the most popular technology due to its established advantages such as low cost, compactness, and easy integration with integrated circuit technology. The most used sensing material in the metal-oxide gas sensors is SnO_2 thin film, as reported to detect several industrial gases such as methane, H_2, CO, H_2S, and methanol [5, 6]. Metal-oxide gas sensors work at high temperature using additional electrical power to supply the heater. Another electrochemical technology based on polymer/carbon nanotube nanocomposites was introduced to allow measurement at room temperature [7]. Gravimetric transduction employs piezoelectric technique, usually known as the quartz crystal microbalance (QCM), for sensitive mass measurement by observing the change of oscillating frequency upon adsorption of the odorants on the crystal surface. For example, Ding et al. reported a QCM-based device coated with copper(II) tetra-*tert*-butyl-5,10,15,20-tetraazaporphyrin that is sensitive to hydrocarbon gases, i.e., hexane, benzene, and toluene [8].

Organic semiconductor materials such as MP and MPc can work as gas sensor based on the change in electrical or optical properties via charge transfer on their surface. The possible sites for gas adsorption were found at the central metal atom and the conjugated π-electron system. It was found that MP and MPc are very versatile sensing materials for detection of a wide range of gases. For example, four metallo-octaethyl porphyrins (with the metal atoms of Mn, Fe, Co, and Ru) thin films were tested with four vapor samples such as 2-propanol, ethanol, acetone, and cyclohexane by recording the reflected light intensity before and after being exposed toward volatiles samples [9]. Blending of MP and MPc also leads to enhancement of the sensor, as reported by Spadavecchia and co-workers [10]. In their work, Zn(II) tetra-4-(2,4-di-*tert*-amylphenoxy)-phthalocyanine and Cu(II) tetrakis (*p*-*tert*-butylphenyl) porphyrin blended thin film was used as the sensing materials for detection of methanol, ethanol, and isopropanol vapors. Spadavecchia et al. also proposed a very novel technique based on the optical absorption using MP and MPc as sensing materials, in which it employs only one sensor film to detect and classify several gases depending on their selectivity on specific wavelength regions. Many research works have reported that MP and MPc are very effective sensing materials for optical sensing due to their versatile and tunable spectra based on variation of central metal and substituent of the molecules [11, 12].

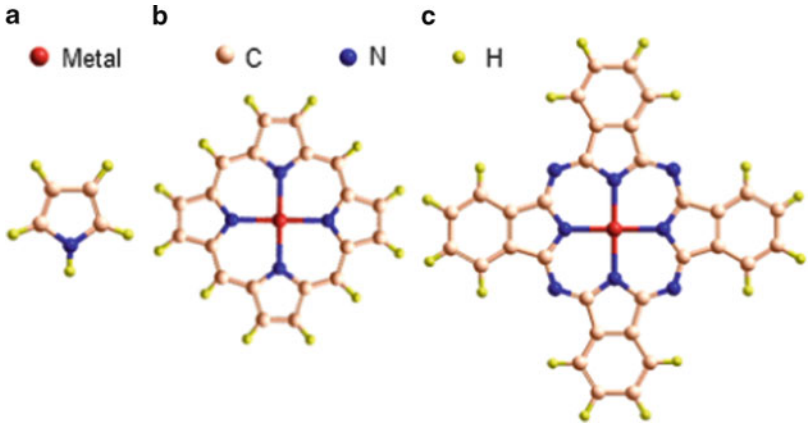

Fig. 1 The molecular structure of (**a**) pyrrole, (**b**) metallo-porphyrin, and (**c**) metallo-phthalocyanine

3 Background of Porphyrin and Phthalocyanine

Porphyrin and phthalocyanine are organic compounds that present the strong absorption spectra in the UV–Vis regions. Both porphyrin and phthalocyanine are therefore used as common coloring compounds in the dye industry.

The structures of porphyrin and phthalocyanine basically consist of four pyrrole units that produce a macrocycle as shown in Fig. 1a. The electronic structures of both organic compounds can be varied by substitution of some peripheral positions with side chains or replacement to the central atom with other metallic atoms (see in Fig. 1b, c). MP and MPc present different electronic properties because of a little but significant variation in the core molecular structures. The skeleton of MP has an extended conjugation system with 24-π electrons leading to a wide range of wavelengths for light absorption. MP presents the strong absorption spectra in a region around 400 nm so-called Soret band or B band. The strong absorption band in UV–Vis region had generally been interpreted in terms of π–π* transition between bonding and anti-bonding molecular orbital [13, 14]. MPc presents the absorption in two regions, e.g., around 300 and 700 nm. The first absorption band (around 300 nm) is described as the transition of π-electron from the highest occupied energy level to the lowest unoccupied level. The maximum absorption band (around 700 nm) is produced from the resonating of π-electrons, which is the free electron gas between two equivalent limiting structures [15].

Computational method based on density functional theory (DFT) at the B3LYP/6-31G* level of theory was used to describe the interaction energies between magnesium-tetra-phenyl-porphyrin (MgTPP) and gas molecules such as methanol, ethanol, isopropanol, acetone, and acetic acid molecules.

Figure 2 plots the interaction energies between gas molecules and MgTPP versus varying distance between the oxygen atom in gas molecule and the Mg atom in

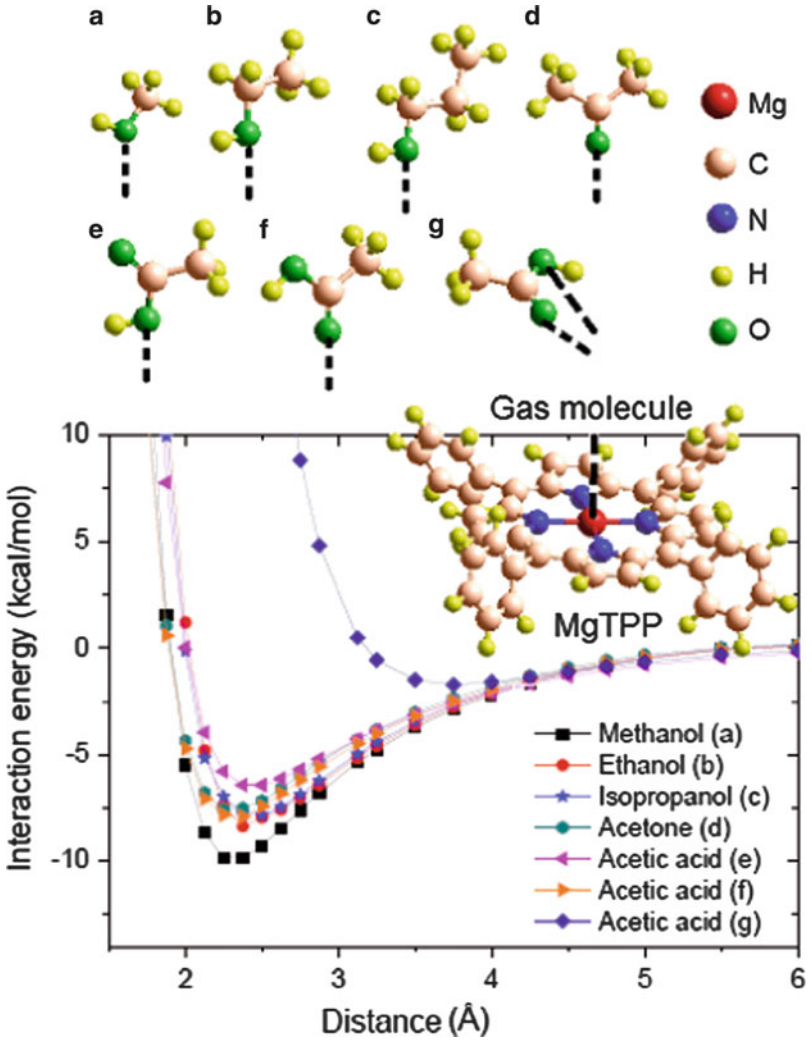

Fig. 2 Plot of interaction energies versus distance between oxygen atom in gas molecule and Mg atom in MgTPP molecule

porphyrin molecule. The interaction energies at the optimized distance indicate that MgTPP presents the stable structure with gas molecules. The results reveal that MgTPP has stronger interaction with methanol molecule at the optimized distance of 2.375 Å than other molecules.

Effect from the substitution on the central metal atom in porphyrin was tested by DFT calculation. The interaction energies *(E_{Int})*, changes in energy gap (ΔE_g), and changes in NBO charges of MTPP (M = Mg, Zn) were investigated as presented in Table 1. The interactions between porphyrin and VOC molecules are determined by the metal atom site via the interactions of the π-electrons and the free electrons of

Table 1 The interaction energies; E_{Int} (kcal/mol) at the optimized distance; D (Å), change in energy gap (MgTPP = 2.82 eV and ZnTPP = 2.91 eV); ΔE_g (eV), and the change in NBO charge: for MgTPP at magnesium (1.70153 a.u.), nitrogen (−0.73441 a.u.); for ZnTPP at zinc (1.61282 a.u.), nitrogen (−0.71875 a.u.); for VOCs at oxygen atomic site (methanol; O −0.741 a.u., ethanol; O −0.759 a.u. and isopropanol; O −0.753 a.u., acetone; O −0.540 a.u. and acetic acid; O −0.591 a.u.) atomic site [16]

				Delta NBO charge of		
Interaction of	D (Å)	E_{Int} (kcal/mol)	ΔE_g (eV)	Metal	O	N
MgTPP with						
Methanol	2.375	−9.92	0.105	+0.001	−0.045	+0.024
Ethanol	2.50	−8.37	0.098	+0.002	−0.041	+0.022
Isopropanol	2.25	−7.83	0.102	+0.003	−0.040	+0.023
Acetone	2.375	−7.61	0.117	+0.001	−0.065	+0.028
Acetic acid (Fig. 2f)	2.375	−7.91	0.099	+0.004	−0.060	+0.026
ZnTPP with						
Methanol	2.375	−5.79	0.121	+0.036	−0.046	+0.010
Ethanol	2.50	−5.66	0.104	+0.031	−0.035	+0.007
Isopropanol	2.50	−5.97	0.103	+0.031	−0.039	+0.010
Acetone	2.50	−4.08	0.109	+0.034	−0.047	+0.010
Acetic acid (Fig. 2f)	2.50	−3.89	0.114	+0.034	−0.048	+0.011

the metal atom in porphyrin with the electrons of the VOC molecules. Hence, electron transfer from the metal atom in porphyrin to an oxygen atom of the VOCs molecule occurs when MgTPP/ZnTPP are in contact with the VOC molecule at the optimized distance [16].

To use MP and MPc as optical gas sensor, the materials have been fabricated as the thin solid film on glass substrate. Measuring changes in the absorption or emission spectra of the thin film is a convenient technique for the optical gas sensor. Various derivatives of MP and MPc compounds have been fabricated to use as the gas sensors. For instance, zinc-5,10,15,20-tetra-phenyl-21H,23H-porphyrin (ZnTPP), manganese(III)-5,10,15,20-tetraphenyl-21H,23H-porphyrin chloride (MnTPPCl), and zinc-2,9,16,23-tetra-*tert*-butyl-29H,31H-phthalocyanine (ZnTTBPc) were widely used to detect NO_2 [17, 18], VOCs, [19] and foods [20]. Figure 3 illustrates the molecular structure of (a) ZnTPP, (b) MnTPPCl, and (c) ZnTTBPc.

4 e-Nose System Based on UV–Vis Spectrophotometer

An optical e-nose system consists of three basic components: a light source, sensing materials or gas sensor, and a detector. In this system, a UV–Vis spectrophotometer was used as the light source and light detector. All measurements were performed at room temperature and at the normal incidence of the light beam. The gas sensing of the organic thin films has been measured under the dynamic gas flow through a home-built stainless steel chamber, equipped with quartz windows for optical measurements as shown in Fig. 4. The carrier gas (in this case 99.9% nitrogen)

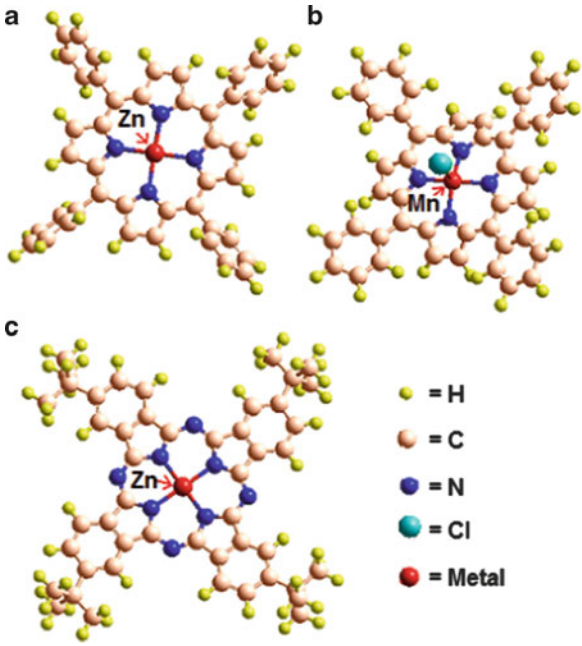

Fig. 3 Molecular structures of (**a**) ZnTPP, (**b**) MnTPPCl, and (**c**) ZnTTBPc

was supplied into the sample bottle that was immersed in a heat bath. The sample vapor was evaporated from the surface of the liquid sample and carried by the nitrogen gas. The gas flow was controlled by solenoid valve to switch between the reference gas and the sample gas every 10 min. The rate of gas flow was controlled by the flow meter. The absorption spectra of the organic thin film were collected by the UV–Vis spectrometer for every 1 s based on the function of the DAQ card.

Figure 5 shows the architecture of a data processing system of this optical e-nose system, starting with a flow of different VOC vapor into the gas sensor that fabricated from MP and MPc compounds. Then the absorption spectra from the UV–Vis spectrophotometer were collected for different sample vapors, comparison with the spectra of the unexposed films. The features extracted from the sensing signal were prepared for further pattern recognition process (in this case, PCA). Then the new data set was presented in the new orthogonal axes or principal components (PCs) such as the first PC (PC1) and the second PC (PC2), which are linear combinations of the original axes. The first PC carries most of the data variance, hence the most important information about the data [12].

5 Development of Optical Gas Sensor

To fabricate the optical gas sensor, MP and MPc must be deposited in the form of solid thin film. There are many fabrication techniques for preparing the thin film, for example, solvent casting, Langmuir–Blodgett, self-assembled monolayer,

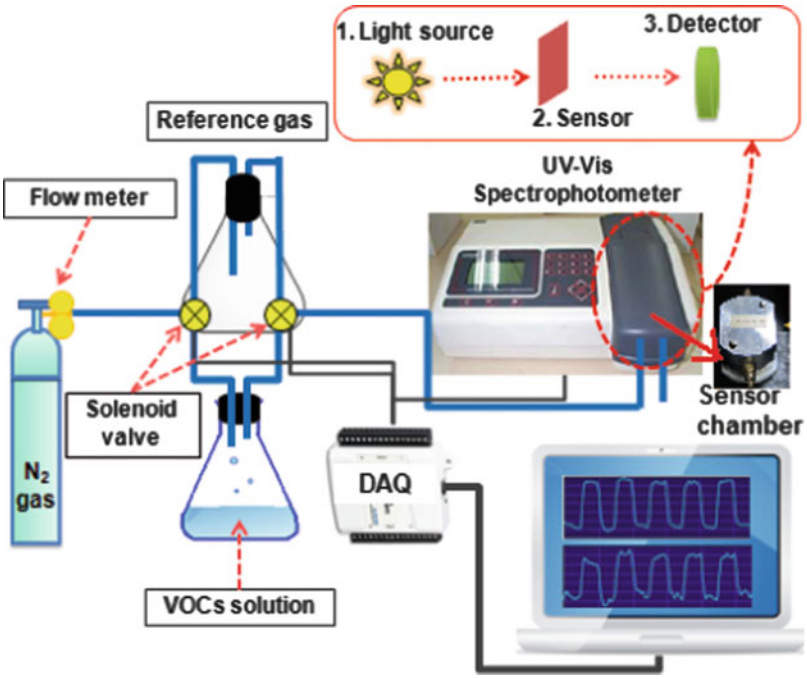

Fig. 4 Schematic diagram of the UV–Vis spectrophotometer setup

electropolymerization, and spin-coating techniques [21–23]. Among these fabrication techniques, spin-coating has been the cost-effective technique to produce regular sensing layers with moderately controllable thickness [24]. Therefore, spin-coating has been widely applied in the field of sensor technology.

In this work, the optical gas sensor uses standard UV–Vis spectrophotometer to measure absorption change when the sensing thin film interacts with the sample vapor. The absorption spectra were divided into several regions based on the response to VOCs. Thus, each sensing material yields different response at different spectral regions [3]. For example, the absorption spectra of MgTPP can be divided into six regions (R) such as R1: 300–370, R2: 370–410, R3: 410–490, R4: 490–555, R5: 555–610, and R6: 610–800 nm. For ZnTPP, the spectra can be divided into R1: 300–360, R2: 360–425, R3: 425–460, R4: 460–550, R5: 550–615, and R6: 615–800 nm) [16]. The gas sensing responses (S) can be calculated from Eq. (1):

$$S = \Delta A / A_{\text{Base}} \tag{1}$$

where ΔA is the difference of the integrated area within a specific range of absorption spectra between the sample (A) and reference (A_{Base}).

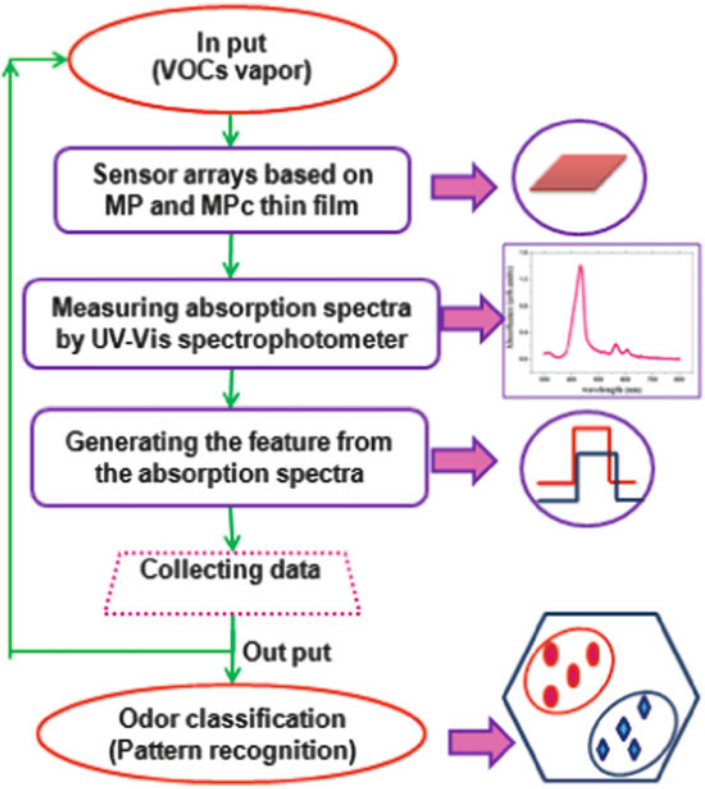

Fig. 5 The architecture of a data processing system for the optical electronic nose

5.1 The Effect of Thickness in Gas Sensor Thin Film

To prepare an efficient chemical gas sensor, the thickness of the thin film must be controlled and optimized. The thickness of the film depends on the concentration of the solution and the spin speed of spin-coating. Hence, the effect of spin speed to the MgTPP spin-coated thin film was tested by using methanol and ethanol vapors as the analyte gases [25]. In this experiment, MgTPP was prepared by spin-coating at the spin speeds of 500, 1,000, and 1,500 rpm and subjected to thermal annealing process. MgTPP thin films spun at lower speed have higher thickness, as revealed by atomic force microscopy. For instance, a typical thickness of the film spun at 500 rpm is 600 nm which decreases to 400 and 200 nm when the rotation speed increases to 1,000 and 1,500 rpm, respectively. Specifically, the spinning speed of 1,000 and 1,500 rpm produces stable thin films that yield almost equivalent sensing properties as shown in Fig. 6.

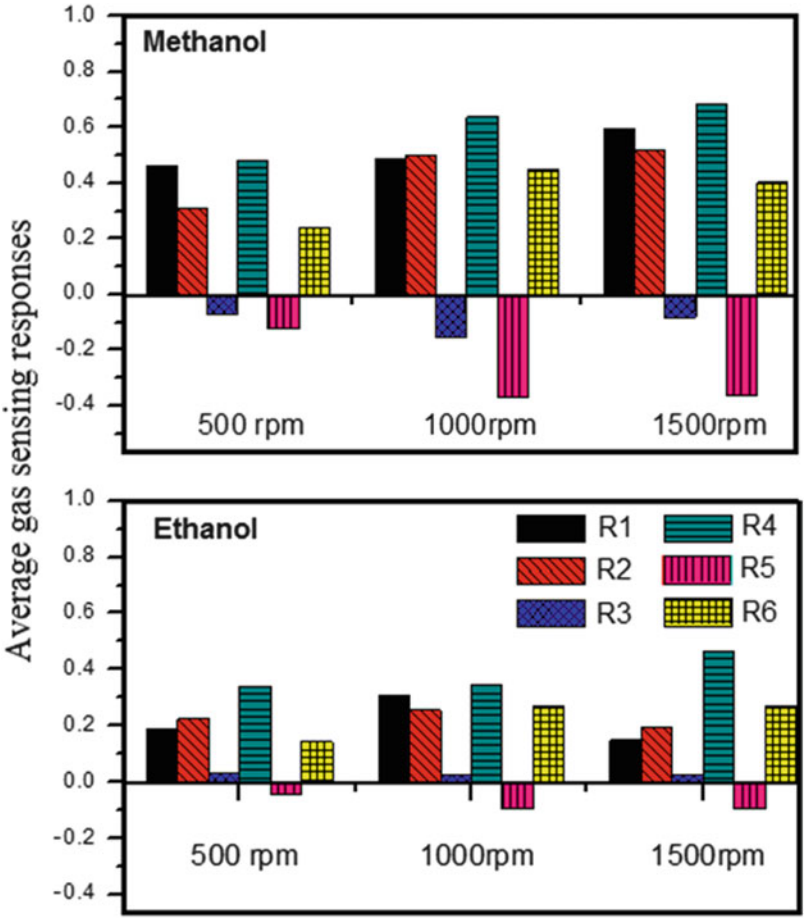

Fig. 6 The average gas sensing responses of MgTPP thin films with methanol and ethanol vapors by varying the speed of spin-coating

5.2 The Effect of Treatment Process in Gas Sensor Thin Film

There have been many research that report the processes to increase the sensitivity of gas sensors such as thermal treatments of cobalt–porphyrins–SnO_2 thin film [26] and solvent-vapor treatments of aluminum phthalocyanine chloride and lead phthalocyanine thin films [27, 28]. Thus, MgTPP thin films undergoing different treatments, i.e., thermal and solvent-vapor treatments were compared in the sensing properties to methanol and ethanol vapors [29]. In Fig. 7, the AFM results indicate larger grain sizes for both treated films, which result from molecular crystallization. The average roughness of the spin-coated film was about 2.83 nm. After thermal and solvent-vapor treatments, the grain size is 41.7 and 41.4 nm, respectively.

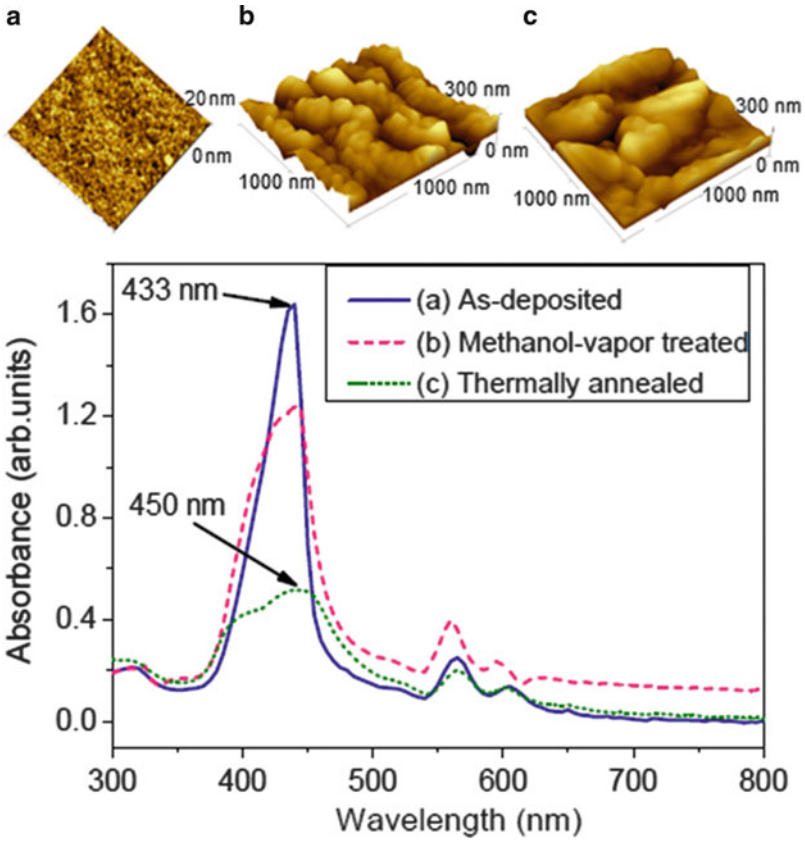

Fig. 7 UV–Vis absorption spectra and AFM images of the spin-coated thin film (spun at 1,000 rpm and concentration of 10 mg/mL) of (**a**) as-deposited, (**b**) methanol-vapor treated, and (**c**) thermally annealed MgTPP thin film

The UV–Vis absorption spectra of these thin films are shown in Fig. 7. The intensity of the main peak of the as-deposited MgTPP thin film located at 433 nm reduced after the film treatment.

In Fig. 8, it can be seen that both types of treated MgTPP films present a good sensing response with methanol for all six ranges, whereas the thermally treated film is more efficient to detect all types of VOCs, namely, methanol and ethanol.

5.3 The Effect of Central Metal Atom in Porphyrin

The effect of central metal atom in porphyrin has been interested by many research, e.g., molecular modeling of Mg- and Zn-porphyrins. The calculation results confirm that the optimized structures of these porphyrins are dependent on the central metal atomic size [30].

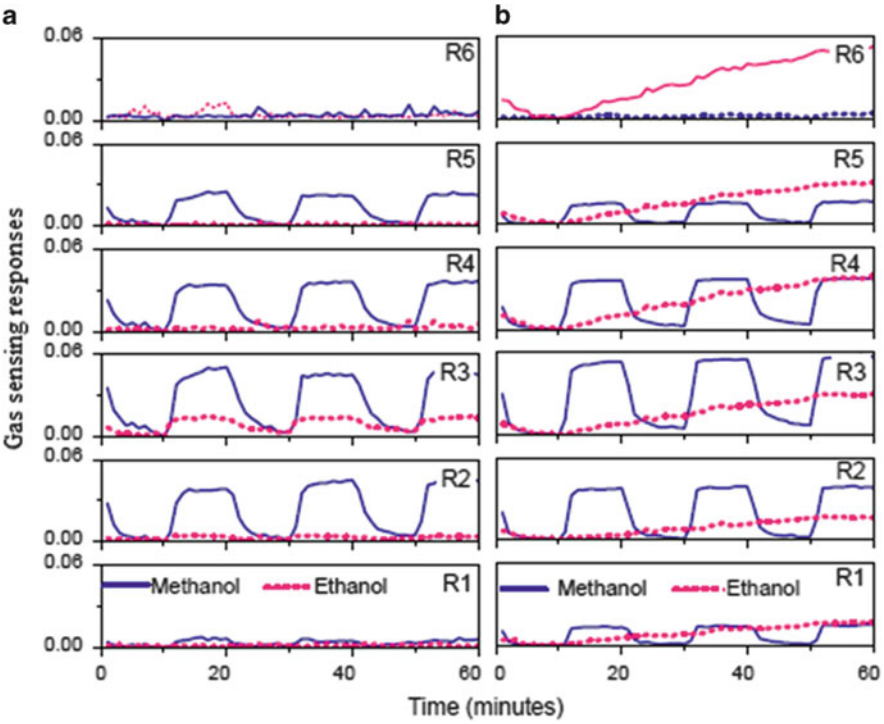

Fig. 8 The gas sensing responses (*S*) of MgTPP films under switching sample/reference gases, (**a**) thermally treated film, and (**b**) methanol-vapor treated film (R1: 300–360 nm, R2: 360–425 nm, R3: 425–510 nm, R4: 510–600 nm, R5: 600–650 nm, R6: 650–800 nm)

The effect of the central metal atom in porphyrin gas sensor was investigated experimentally as shown in Fig. 9. In this experiment, it was shown that both MgTPP and ZnTPP films express more sensing response to methanol than other alcohols. It can be seen that MgTPP is more selective to methanol comparing to ZnTPP. Thus, ZnTPP expresses higher response to ethanol and isopropyl alcohol than MgTPP [16].

5.4 The Hybrid Gas Sensor by Mixed Layer MP and MPc

The spin-coated thin films of MP and MPc are widely used as opto-chemical sensing materials because of their absorbance in the UV–Vis regions and their absorption spectral changes upon exposure to various vapor such as alcohols [24], amines, hexylamine, and octylamine [31]. The strongest response for porphyrin gas sensors corresponds to the Soret band or main peak of absorption spectra, indicating the π–π^* transition between bonding and anti-bonding molecular orbital in the porphyrin compounds [32]. Thus, the hybrid gas sensor between MP and MPc has

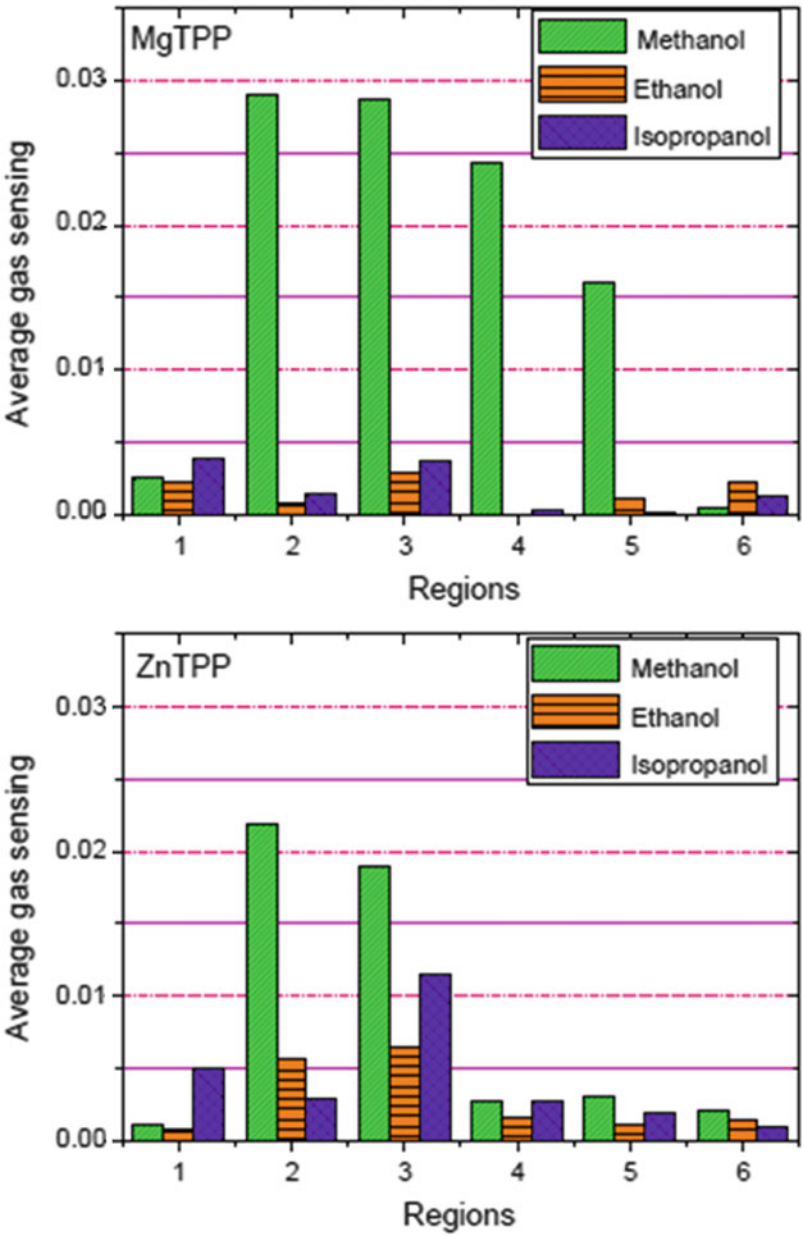

Fig. 9 The average gas sensing of MgTPP annealed film and ZnTPP spin-coated film

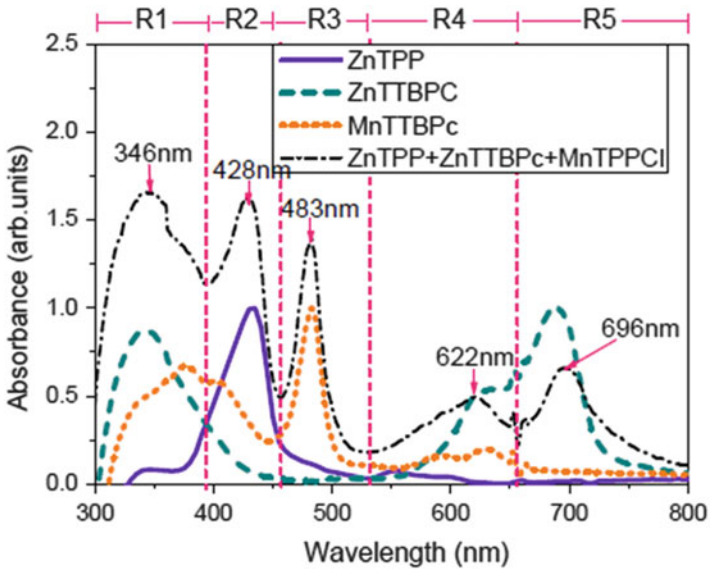

Fig. 10 Optical absorption spectra of (**a**) the ZnTTBPc, ZnTPP, and MnTPPCl spin-coated film and (**b**) the mixed layer of ZnTTBPc/ZnTPP/MnTPPCl spin-coated film

been investigated because MP and MPc present the main peak of absorption spectra in the different wavelength regions. To prepare the hybrid gas sensor thin film, ZnTPP, MnTPPCl, and ZnTTBPc were obtained from Sigma-Aldrich. The mixed solution of ZnTPP/MnTPPCl/ZnTTBPc was obtained from a 3 mL of chloroform solution that was composed of 5 mg of ZnTPP, 10 or 15 mg of MnTPPCl, and 12 mg of ZnTTBPc. Then the blended ZnTPP/MnTPPCl/ZnTTBPc spin-coated thin films were obtained by spinning at 1,000 rpm for 30 s. The optical absorption spectra of thin films were recorded by the e-nose setup (Fig. 4).

The absorption spectra of the ZnTTBPc/ZnTPP/MnTPPCl spin-coated thin films are shown in Fig. 10. The hybrid thin films show main peaks at 346, 428, 483, 622, and 696 nm, in accordance with the main peaks of the MP and the MPc. Then we divided the absorption spectra into five regions around each of the main peaks: 300–400 (R1), 400–460 (R2), 460–530 (R3), 530–655 (R4), and 655–800 nm (R5).

Figure 11a shows the average gas sensing of ZnTTBPc, ZnTPP, and MnTPPCl spin-coated thin films to 10 mol% of alcohols vapor in the nitrogen gas. The concentration of alcohols vapor was controlled by the heat bath and calculated from the weight loss of the alcohols in the sample bottles. Methanol shows the highest sensing response amongst the alcohols. ZnTPP and MnTPPCl exhibit no response to ethanol and isopropanol alcohol in the region R3. The hybrid layer of ZnTTBPc/ZnTPP/MnTPPCl displays responses to all types of alcohols as shown in Fig. 11b, c. Overall the results indicate that the hybrid spin-coated thin films fabricated from 12 mg of ZnTTBPc, 5 mg of ZnTPP, and 15 mg of MnTPPCl in a 3 mL of chloroform show the good sensing response with alcohol vapor.

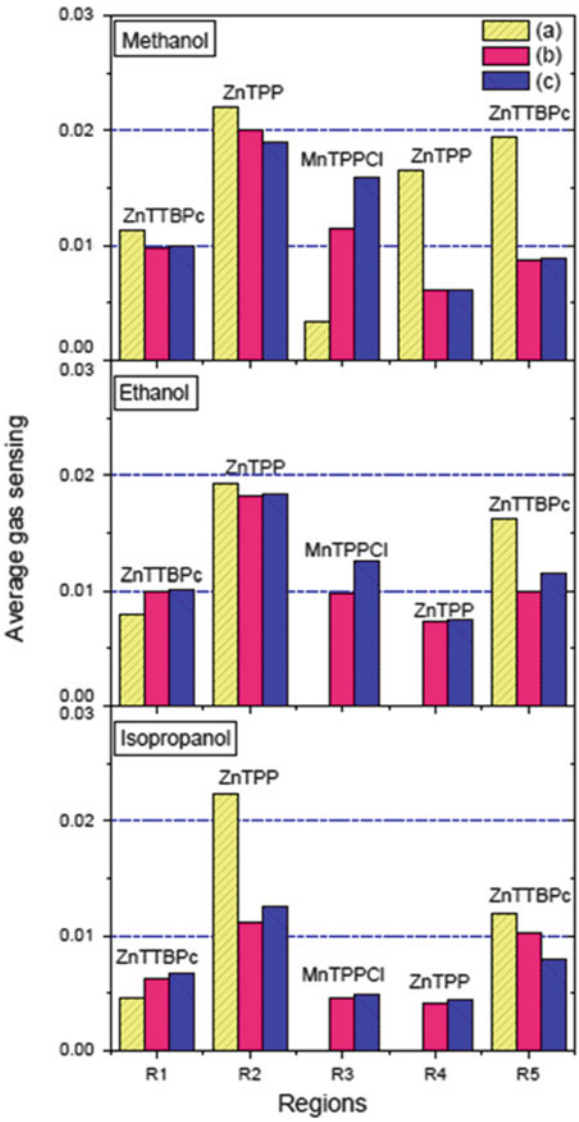

Fig. 11 The average gas sensing of (**a**) ZnTTBPc, ZnTPP, and MnTPPCl, (**b**) hybrid layer of ZnTTBPc: ZnTPP:MnTPPCl (12:5:10) and (**c**) hybrid layer of ZnTTBPc:ZnTPP:MnTPPCl (12:5:15) spin-coated thin film

6 Odor Classification Based on PCA

The PCA is a multivariate data analysis method that has been widely used as a pattern recognition algorithm in most e-nose systems to discriminate different VOCs, e.g., alcohols, toluene, methylethylketon, soft drinks, and alcoholic beverages [33–35].

Figure 12 shows PCA plots in the two dimensions as related to the sensing signal from the hybrid layer of ZnTTBPc/ZnTPP/MnTPPCl spin-coated thin film based on

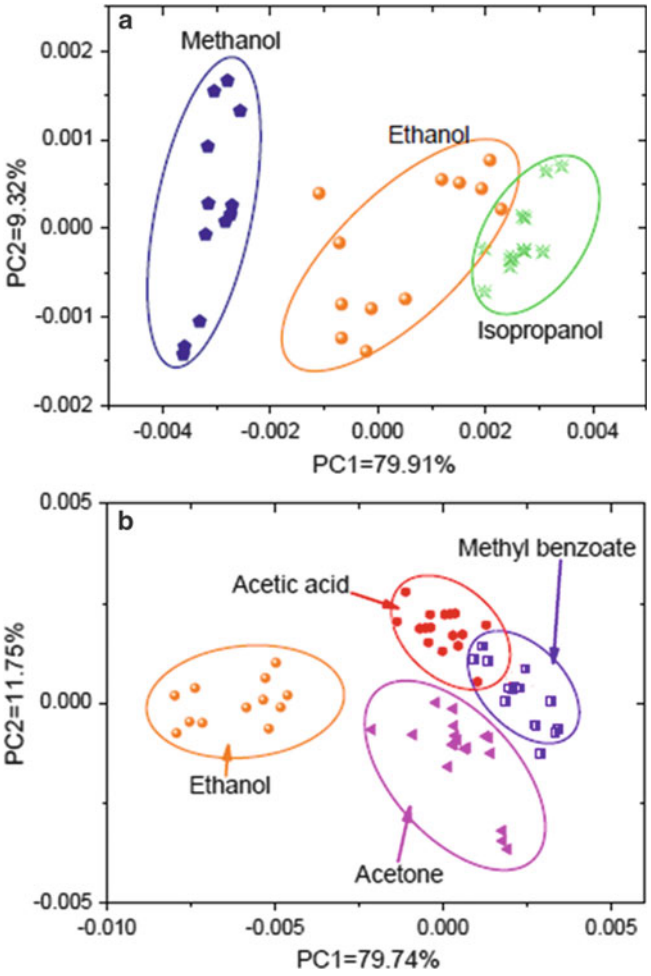

Fig. 12 PCA two-dimensional score plot related to the five arrays of hybrid gas sensor corresponding to (**a**) three types of alcohol vapor and (**b**) VOCs vapor

the optical absorption technique [36]. The results show that these hybrid materials can classify three types of alcohol, namely, methanol, ethanol, and isopropanol (Fig. 12a). These optical sensors separate the ethanol vapor from the other VOCs, methyl benzoate, acetone, and acetic acid (Fig. 12b). Furthermore, the classification of the different volume of ethanol in water was tested with the hybrid gas sensor. The ratios between ethanol and water were varied by changing the volume of ethanol and in water. The PCA calculation can separate the different volume of ethanol and in water from 0% to 100% (see Fig. 13).

The separation between 0% and 100% ethanol is shown clearly in PC1 axis direction. The PC1 axis, which is the highest variance value of principal coordinates

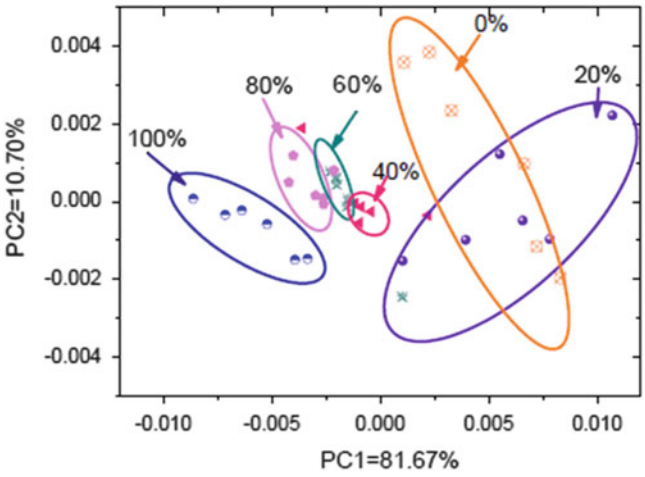

Fig. 13 PCA two-dimensional score plot related to the five arrays of hybrid gas sensor corresponding to the concentration of ethanol in water

(81.67%), represents the most important information of the data set [37]. The data set of 100% ethanol is located at the left-hand side of Fig. 13 while the data set of 0% ethanol (or 100% water) is located at the right-hand side of Fig. 13. It can be concluded that PCA is an effective statistical method in the electronic nose system to classify the group of odor. This method presents a high efficiency and a low demand on computing power in the system. Consequently, these results confirm that the optical electronic nose system based on the three types of organic compounds should be highly effective for discriminating VOCs and applicable to qualitative measurements of foods and beverages.

Acknowledgments Mahidol University and National Nanotechnology Center (Project No. P-12-01157) are acknowledged for supports.

References

1. Manno D, Micocci G, Serra A et al (1999) Gas sensing properties of meso, meso-buta-1,3-diyne-bridged Cu(II) octaethylporphyrin dimer Langmuir-Blodgett films. Sens Actuators B Chem 57:179–182
2. Montmeat P, Madonia S, Pasquinet E et al (2005) Metalloporphyrins as sensing material for quartz-crystal microbalance nitroaromatics sensors. J Sens IEEE 5:174–179
3. Uttiya S, Pratontep S, Bhanthumnavin W et al (2008) Volatile organic compound sensor arrays based on zinc phthalocyanine and zinc porphyrin thin films. In: Proceedings of the 2nd IEEE-NEC 2008, pp 618–623
4. Pearce TC, Schiffman SS, Nagle HT et al (2003) Handbook of machine olfaction electronic nose technology. Wiley-VCH Verlag GmbH & Co. KGaA, Weinheim

5. Campbell M (1997) Sensor system for environmental monitoring, vol 1: sensor technologies. Blackie Academic & Professional, London
6. Wongchoosuk C, Wisitsoraat A, Tuantranont A et al (2010) Portable electronic nose based on carbon nanotube-SnO_2 gas sensors and its application for detection of methanol contamination in whiskeys. Sens Actuators B 147:392–399
7. Lorwongtragool P, Wisitsoraat A, Kerdcharoen T (2011) An electronic nose for amine detection based on polymer/SWNT-COOH nanocomposite. J Nanosci Nanotechnol 11:10454–10459
8. Ding H, Erokhin V, Ram MK et al (2000) A physical insight into the gas-sensing properties of copper II tetra-tert-butyl-5,10,15,20-tetraazaporphyrin Langmuir-Blodgett films. Thin Solid Films 379:279–286
9. Akrajas SMM, Yahaya M (2002) Enriching the selectivity of metalloporphyrins chemical sensors by means of optical technique. Sens Actuators B Chem 85:191–196
10. Spadavecchia J, Ciccarella G, Siciliano P et al (2004) Spin-coated thin films of metal porphyrin-phthalocyanine blend for an optochemical sensor of alcohol vapour. Sens Actuators B Chem 100:88–93
11. Muthukumar P, John SA (2011) Highly sensitive detection of HCl gas using a thin film of meso-tetra(4-pyridyl)porphyrin coated glass slide by optochemical method. Sens Actuators B 159:238–244
12. Spadavecchia J, Ciccarella G, Rella R et al (2003) Metallophthalocyanines thin films in array configuration for electronic optical nose applications. Sens Actuators B 96:489–497
13. Smith KM (1975) Porphyrin and metalloporphyrins. Elsevier Scientific Pub. Co., Newyork
14. El-Nahass MM, Zeyada HM, Aziz MS et al (2005) Optical absorption of tetraphenylporphyrin thin films in UV–vis–NIR region. Spectrochim Acta A 61:3026–3031
15. Moser FH, Thomas AL (1963) Phthalocyanine compounds. Reinhold, London
16. Kladsomboon S, Pratontep S, Puntheeranurak T et al (2011) An artificial nose based on M-porphyrin (M = Mg, Zn) thin film and optical spectroscopy. J Nanosci Nanotechnol 11:10589–10594
17. Richardson TH, Dooling CM, Worsfold O et al (2002) Gas sensing properties of porphyrins assemblies prepared using ultra-fast LB deposition. Colloids Surf A 198–200:843–857
18. Li XY, Shen SY, Zhou QF (1998) The gas response behavior of spin-coated phthalocyanine films to NO_2. Thin Solid Films 324:274–276
19. Arshad S, Salleh MM, Yahaya M (2007) Detection of volatile organic compounds using titanium dioxide coated with dye-porphyrins thin films in bulk acoustic system. Solid State Sci Technol 15:175–181
20. Salleh MM, Umar AA, Yahaya M (2002) Optical sensing of capsicum aroma using four porphyrins derivatives thin films. Thin Solid Films 417:162–165
21. Amico AD, Natale CD, Paolesse R et al (2000) Metallo porphyrins as basic material for volatile sensitive sensors. Sens Actuators B 65:209–215
22. Luo T, Zhang W, Gan F (1992) Structural change of Langmuir-Blodgett film of tetra-neopentoxy phthalocyanine zinc during heat treatment. Opt Mater 1:267–270
23. Liu CHJ, Lu WC (2007) Optical amine sensor based on metallophthalocyanine. J Chin Inst Chem Eng 38:483–488
24. Gu Z, Yin J, Liang P et al (2004) Temperature characteristics of optical parameters of phthalocyanine LB films and spin-coated film. Opt Mater 27:1618–1622
25. Kladsomboon S, Pratontep S, Uttiya S et al (2008) Alcohol gas sensors based on magnesium tetraphenyl porphyrins. In: Proceedings of the 2nd IEEE-NEC 2008, pp 952–955
26. Nardis S, Monti D, Natale CD et al (2004) Preparation and characterization of cobalt porphyrins modified tin dioxide film for sensor applications. Sens Actuators B 103:339–343
27. Kato K, Saito Y, Ohdaira Y et al (2006) Evaluation of nanostructure and properties of aluminum phthalocyanine chloride thin films due to ethanol-vapor treatment. Thin Solid Films 499:174–178

28. Ho KC, Chen CM, Liao JY (2005) Enhancing chemiresistor-type NO gas-sensing properties using ethanol-treated lead phthalocyanine thin films. Sens Actuators B 108:418–426
29. Kladsomboon S, Pratontep S, Puntheeranurak T et al (2009) Investigation of thermal and methanol-vapor treatments for MgTPP as an optical gas sensor. In: Proceedings of the 4th IEEE-NEM 2009, pp 843–847
30. Poveda LA, Ferro VR, Garcia de la Vega JM et al (2000) Molecular modeling of highly peripheral substituted Mg- and Zn-porphyrins. Phys Chem Chem Phys 2:4147–4156
31. Dunbar ADF, Richardson TH, McNaughton AJ et al (2006) Investigation of free base, Mg, Sn, and Zn substituted porphyrin LB films as gas sensors for organic analytes. J Phys Chem 110:16646–16651
32. Zhang X, Zhang Y, Jiang J (2005) Infrared spectra of metal-free, N,N-dideuterio, and magnesium porphyrins: density functional calculations. Spectrochim Acta A 61:2576–2583
33. Fernandez MJ, Fontecha JL, Sayago I et al (2007) Discrimination of volatile compounds through an electronic nose based on ZnO SAW sensors. Sens Actuators B 127:277–283
34. Zhang C, Suslick KS (2007) Colorimetric sensor array for soft drink analysis. J Agric Food Chem 55:237–242
35. Zhang C, Bailey DP, Suslick KS (2006) Colorimetric sensor arrays for the analysis of beers: a feasibility study. J Agric Food Chem 54:4925–4931
36. Kladsomboon S, Pratontep S, Kerdcharoen T (2010) Optical electronic nose based on porphyrin and phthalocyanine thin films. In: Proceedings of the ECTI 2010, pp 565–568
37. Brereton RG (2003) Chemometrics data analysis for the laboratory and chemical plant. Wiley, England